



**HAL**  
open science

# Numerical dosimetry of ELF induced currents in the human body : impact of post-processing on a benchmark and on a realistic case

Jean-Pierre Ducreux, Yves Guillot, Pierre Thomas, Noël Burais, Riccardo Scorretti, Laurent Krähenbühl, Laurent Nicolas

## ► To cite this version:

Jean-Pierre Ducreux, Yves Guillot, Pierre Thomas, Noël Burais, Riccardo Scorretti, et al.. Numerical dosimetry of ELF induced currents in the human body : impact of post-processing on a benchmark and on a realistic case. EHE'09: International Conference on Electromagnetic Fields, Health and Environment, Nov 2009, São Paulo, Brazil. hal-00435205

**HAL Id: hal-00435205**

**<https://hal.science/hal-00435205>**

Submitted on 3 Dec 2009

**HAL** is a multi-disciplinary open access archive for the deposit and dissemination of scientific research documents, whether they are published or not. The documents may come from teaching and research institutions in France or abroad, or from public or private research centers.

L'archive ouverte pluridisciplinaire **HAL**, est destinée au dépôt et à la diffusion de documents scientifiques de niveau recherche, publiés ou non, émanant des établissements d'enseignement et de recherche français ou étrangers, des laboratoires publics ou privés.

# Numerical dosimetry of ELF induced currents in the human body: impact of post-processing on a benchmark and on a realistic case

Jean-Pierre Ducreux\*, Yves Guillot\*, Pierre Thomas\*, Noel Burais<sup>♥</sup>, Riccardo Scorretti<sup>♥</sup>, Laurent Krähenbühl<sup>♣</sup>, Laurent Nicolas<sup>♣</sup>

\* LAMEL- EDF R&D, 1 avenue du Général de Gaulle, 92141 Clamart, France

<sup>♥</sup> CNRS, UMR 5005, Laboratoire Ampère, Ecully, F-69134, France; Université de Lyon, Lyon, F-69361, France. Université Lyon 1, Villeurbanne, F-69622, France.

<sup>♣</sup> CNRS, UMR 5005, Laboratoire Ampère, Ecole Centrale de Lyon, Ecully, F-69134, France

**Abstract**— Numerical dosimetry is widely used to demonstrate compliancy to regulation. There are several possible approaches but whatever the method is, an appreciation of the numerical imperfections is required. We proposed here a geometrical criterion on the finite element mesh. We applied this method on an academic benchmark to demonstrate the efficiency and the sensitivity of numerical methods to this criterion, then on a human phantom in order to check mesh quality. Computations are performed on three software. Results show a good agreement between some results. However there is a great discrepancy on some organs.

**Index Terms**— Biological effects, numerical dosimetry, Finite Element method.

## I. INTRODUCTION

THE current density computation inside human bodies to demonstrate compliance to regulation [1] is a challenging problem for computational electromagnetism because no measurements are available as reference to validate these results. A lot of works with different formulations to solve Maxwell’s equations have tried to build models and perform computations. So several methods, formulations and computational phantoms have been proposed since early 80s [2], [3], [4]. We can mention impedance method [5], Finite Difference Time Domain method (FDTD) in quasi static domain, Scalar Potential Finite Difference method (SPFD) [6], Finite Element Method [3] or some methods mixing the above mentioned ones [4].

When dealing with numerical dosimetry it is important to establish on one hand the reliability of the computational code, and on the other hand the accuracy of the computational phantom. In this work, we focus on the first aspect (reliability of computational codes). As far as we know no systematic comparison between these methods have been performed

using the same benchmarks. In order to estimate the influence of mesh quality on computed results, we chose to work on an academic benchmark. For this study there exists an analytical expression for the maximum of the induced current density. Some academic and commercial Finite Element codes have been tested with this benchmark. We show some results obtained with different tools and methods using the same mesh. We use a coarse and a fine mesh, and we present the results obtained with and without filtering “bad elements” (in the sense which is defined in next sections) away in the post-processing. Finally we show here some results obtained with the same anatomical computational phantom.

## II. BENCHMARK ANALYSIS

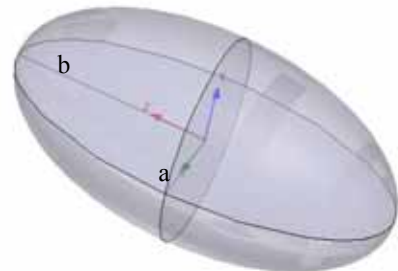


Fig. 1. Description of the ellipsoid – Definition of major axis (b) and minor axis (a) in case of flux source along y -axis

This benchmark is based on the computation of induced currents in a conductive spheroids ( $\sigma = 0.2$  S/m). The source field is uniform in space and vary sinusoidally in time ( $B_{\text{eff}} = 500 \mu\text{T}$  along spheroid axis y). In cylindrical coordinates, the analytical expression of the maximum induced current density  $J$  is given by:  $J_{\text{max}} = 2\sigma\pi f B \cdot ab^2 / (a^2 + b^2)$ , where  $\sigma$  is the conductivity,  $f$  the frequency,  $2a$  and  $2b$  are the minor and major axes of the ellipse perpendicular to the induction axis (cf. Figure 1). Some approaches to appreciate mesh quality are proposed in [7]. We chose here to analyse the mesh quality with a geometrical criterion. For each tetrahedron, two particular spheres can be defined. The first one is the insphere

that is tangent to the faces. The second one is the circumscribed sphere that touches each tetrahedron's vertex. In Figure 2, in case of a very flattened tetrahedron (right), the largest sphere is the circumscribed sphere and the gray one is the insphere. The ratio between the radius  $R_{int}$  of the first sphere and the radius  $R_{ext}$  of the second one is chosen here as a criterion of mesh quality. It means that post-processing will be only performed on tetrahedral elements with a good criterion (more than 10% – namely  $q = 3R_{int}/R_{ext} > 0.1$ ).

For several spheroid sizes as in [8], we compute the current density with a coarse mesh and a fine mesh. The aim of the computation is to calculate the maximum induced current density inside the spheroid. Depending on the formulation (A-

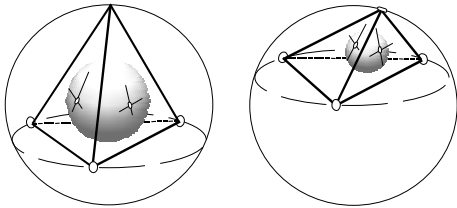


Fig. 2. Representation of circumscribed sphere and insphere

V, T- $\omega$  or  $\phi$ -A), the numerically computed current density is more or less sensitive to mesh quality. Table 1 summarizes results for a magnetic induction along y-axis for three sizes of ellipsoid with a coarse mesh. The reference is given by analytical solution. For each code or formulation the first value indicates the maximum current level computed with all tetrahedral. The value between parentheses indicates the maximum current level computed only with the tetrahedral satisfying the geometrical criterion. One observes that the results obtained with a coarse mesh are heavily formulation dependant, whereas this is not the case with a finer mesh (data not shown).

### III. CONCLUSION: APPLICATION TO AN ANATOMICAL PHANTOM

The human body model was provided by ANSOFT (cf. figure 3). Eventhough this geometrical model is available with

TABLE I

MAX. INDUCED CURRENTS COMPUTED WITH A COARSE SPHEROID (mA/m <sup>2</sup> )					
Size	Reference	$\phi$ -A	A-V	T- $\omega$	Maxwell 3D
60 × 30	5.33	7.50	8.29	5.46	4.87
		(6.10)	(5.29)	(5.46)	(3.40)
120 × 60	10.66	18.20	23.47	12.14	19.72
		(14.60)	(11.42)	(12.14)	(14.75)
180 × 80	14.84	24.70	46.99	9.52	29.03
		(16.10)	(15.30)	(8.23)	(15.98)

Sizes are given in cm. The value computed between parentheses ( ) represent the values obtained by taking into account only "good quality" elements. The numerical results have been obtained with the codes *Gefem++* ( $\phi$ -A), *Carmel* (A-V and T- $\omega$ ) and *Maxwell 3D*.

a 2 mm resolution, ), we decided to use the 4 mm resolution model in order to simplify results analysis. It leads to a 19 organ model; the mesh is composed of 70 000 tetrahedral elements. The induced current is computed by using the

codes *Gefem++* ( $\phi$ -A formulation) and *Carmel* (A-V and T- $\omega$  formulations). It is found that there is a rather good agreement for some organs, mainly those with a low conductivity. But there are also great discrepancies on other organs, mainly those with high conductivity, notably the eyes. On these organs, the filtering with a geometrical criterion has no effect as the three corrected methods differ. Conversely, the effect of filtering is important on muscle.

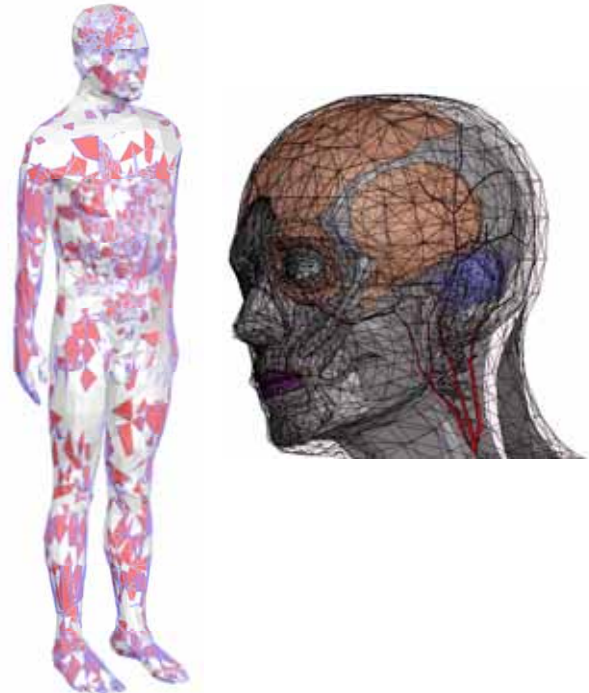


Fig. 3. Left: the computational phantom; the elements eliminated for post-processing are rendered in red. Right: details of the 2mm resolution phantom.

### REFERENCES

- [1] Directive 2004/40/EC of the European Parliament and of the Council of 29 April 2004 on the minimum health and safety requirements regarding the exposure of workers to the risks arising from physical agents (electromagnetic fields). Official Journal of the European Union.
- [2] M.A. Stuchly, O.P. Gandhi, *Bioelectromagnetics* 21 : 167-174 (2000).
- [3] P. Baraton, B. Hutzler: "Magnetically induced currents in the human body", IEC Technology Trend Assessment (1995).
- [4] R. Scorretti, N. Burais, O. Fabregue, A. Nicolas, L. Nicolas "Computation of the induced current density into the human body due to relative LF magnetic field generated by realistic devices", *IEEE Trans. Mag.* vol. 40, no. 2 (2004), pp 643-646.
- [5] O. P. Gandhi, J. F. Deford, H. Kanai, Impedance method for calculation of power depositions patterns in magnetically induced hyperthermia, *IEEE Trans. On Biomed Eng.*, Vol. 31, n° 10, pp 644-651 (19984).
- [6] T. W. Dawson, M. A. Stuchly, Analytic validation of a three dimensional scalar finite difference code for low frequency magnetic induction, *ACES Journal*, Vol. 11, No. 3, pp. 72-81 (November 1996).
- [7] F.-X. Zgainski, "An a priori Indicator of Tetrahedron Finite Element Quality based on the Condition number of the Elementary Matrix", Conference on Electromagnetic Field Computation, Tucson (1998).
- [8] EN50392:2004, "Generic standards to demonstrate the compliance of electronic and electrical apparatus with the basic restrictions related to human exposure to electromagnetic fields" (2004).